European Journal of Pharmaceutical Sciences 44 (2011) 341–350

Contents lists available at SciVerse ScienceDirect

European Journal of Pharmaceutical Sciences

journal homepage: www.elsevier.com/locate/ejps

Investigations on the effect of different cooling rates on the stability of amorphous indomethacin

P. Karmwar [a], J.P. Boetker [b], K.A. Graeser [a], C.J. Strachan [a], J. Rantanen [b], T. Rades [a,*]

[a] School of Pharmacy, University of Otago, 18 Frederick Street, Dunedin 9054, New Zealand
[b] Faculty of Pharmaceutical Sciences, Department of Pharmaceutics and Analytical Chemistry, University of Copenhagen, Universitetsparken 2, 2100 Copenhagen Ø, Denmark

ARTICLE INFO

Article history:
Received 2 May 2011
Received in revised form 28 July 2011
Accepted 15 August 2011
Available online 23 August 2011

Keywords:
TTT diagram
Minimum cooling rate
Glass forming ability
Non-isothermal crystallisation
Physical stability
Amorphous

ABSTRACT

Amorphous forms of indomethacin have previously been prepared using various preparation techniques and it could be demonstrated that the way the material was prepared influenced the physicochemical properties of the amorphous form of the drug. The aim of this study was to use one preparation technique (transformation via the melt) to prepare amorphous indomethacin and to investigate the influence of the cooling rate (as a processing parameter) on the physical stability of the resulting amorphous form. The amorphous materials obtained were analysed for their structural characteristics using Raman spectroscopy in combination with multivariate data analysis. The onset of crystallisation was determined as an indicator of the physical stability of the materials using differential scanning calorimetry (DSC) and polarising light microscopy. The Johnson–Mehl–Avrami (JMA) model and Sestak–Berggren (SB) model were used in this study to describe the non-isothermal crystallisation behaviour.

All differently cooled samples were completely X-ray amorphous. Principal component analysis of the Raman spectra of the various amorphous forms revealed that the samples clustered in the scores plot according to the cooling rate, suggesting structural differences between the differently cooled samples. The minimum cooling rate required to obtain amorphous indomethacin was 1.2 K min^{-1}, as assessed from the time–temperature–transformation (TTT) diagram. The physical stability of the samples was found to increase as a function of cooling rate in the order of 30 K min^{-1} > 20 K min^{-1} > 10 K min^{-1} > 5 K min^{-1} > 3 K min^{-1} ≈ 1.2 K min^{-1} and was in agreement with calculated descriptors for the glass forming ability (GFA), including the reduced glass transition temperature (T_{rg}) and the reduced temperature (T_{red}). The JMA model could not be applied to describe the crystallisation process for the differently cooled melts of indomethacin in this study. The kinetic exponent M from the autocatalytic SB model however, showed a positive correlation with glass stability.

1. Introduction

Solid materials can exist in different polymorphic (crystalline) forms, and amorphous forms (Heinz et al., 2007). In polymorphic materials, the thermodynamically stable form is the primary minimum in the energy landscape and other polymorphs represent higher order minima. In contrast, the amorphous form of a material does not correspond to an energetic minimum (Stillinger and Weber, 1984; Wales, 2010) and no state equations exist to describe an amorphous form. It is therefore not surprising that the use of different preparative approaches to prepare amorphous solids may influence thermal and structural properties of amorphous materials along with their physical stability (Karmwar et al., 2011). We have previously demonstrated that structural and thermal properties (determined by Raman spectroscopy and differential scanning calorimetry (DSC), respectively) of some amorphous drugs (indomethacin, simvastatin) were influenced by the use of different preparation techniques such as quench cooling of the melt, spray drying and milling (Graeser et al., 2009; Patterson et al., 2005). In this study we use only one preparative technique to prepare amorphous solids (melting followed by cooling), but different processing conditions (cooling rates) for the preparation of amorphous forms of the model drug indomethacin. To date, only a limited amount of research has been undertaken into understanding the effect of processing parameters on the physical stability of amorphous drugs (Bhugra et al., 2008; Bøtker et al., 2011; Hancock et al., 2002; Surana et al., 2004).

For amorphous materials prepared by transformation through the melt, there is a thermodynamic driving force to convert the amorphous form into a thermodynamically stable or metastable crystalline form during cooling through the supercooled melt (i.e. in the temperature interval between the melting point (T_m) and

* Corresponding author. Tel.: +64 (3) 479 5410; fax: +64 (3) 479 7034.
E-mail address: thomas.rades@otago.ac.nz (T. Rades).

0928-0987/$ - see front matter © 2011 Elsevier B.V. All rights reserved.
doi:10.1016/j.ejps.2011.08.010

the glass transition temperature (T_g) of the material). The time allowed for the formation of the glass in the supercooled melt may thus be a critical parameter for the stability of the resulting amorphous material.

1.1. Determination of GFA parameters

Identification of the minimum cooling rate (R_c), above which no re-crystallisation occurs during cooling, provides information on the glass forming ability (GFA) of a material. The lower the R_c of the material, the higher the GFA, which results in a higher glass stability (Giordano et al., 2005; Kaushal and Bansal, 2008; Nascimento et al., 2005). The R_c to obtain an amorphous material can be determined from a time, temperature, transformation (TTT) diagram (Woodard et al., 1999). The establishment of a TTT diagram is usually based on DSC measurements and has in the past mostly been used for inorganic systems and determination of the GFA of pharmaceutical materials through calculation of the minimum cooling rate R_c has been limited (Kaushal and Bansal, 2008).

An example of a typical TTT diagram is shown in Fig. 1. The minimum cooling rate R_c is defined as the rate tangential to the locus (''tip of the nose'') of the area at which nucleation and growth of crystals takes place (shaded area in Fig. 1). This area in the TTT diagram typically has a ''nose-shape'' (Denicourt et al., 2003). R_c may be calculated from the TTT diagram as follows:

$$R_c = \frac{T_m - T_n}{t_n} \tag{1}$$

where T_m is the melting point of the material, and T_n and tn are the temperature and time point at the locus, respectively (Denicourt et al., 2003; Hng et al., 1996).

However, the laborious nature to experimentally establish a TTT diagram and general difficulties in measuring R_c accurately (due to nucleating heterogeneities and thermodynamic barriers to nucleation), led to the proposal of various other empirical approaches and numerical descriptors to obtain information on the GFA of a material (Onorato and Uhlmann, 1976). The majority of these are based on thermal events such as the glass transition temperature (T_g), crystallisation temperature (T_c) and melting temperature (T_m) of the material.

The reduced glass transition temperature (T_{rg}) can be used to assess the GFA of a material (Kauzmann, 1948; Turnbull, 1969) and can be calculated as follows:

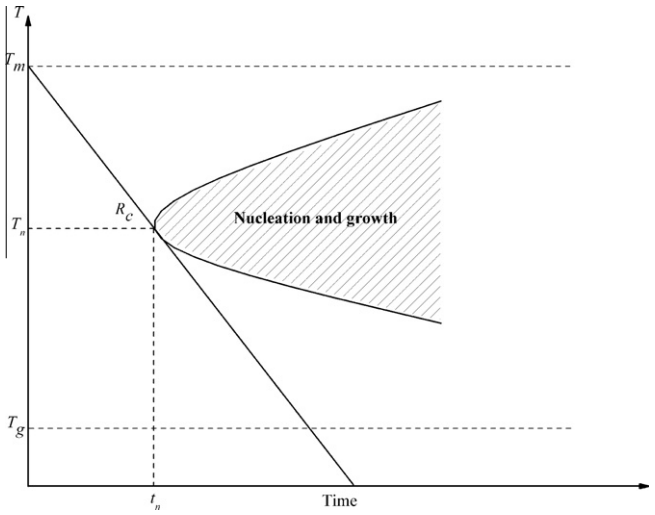

Fig. 1. Annotated time–temperature–transformation diagram, showing the minimum cooling rate to avoid crystallisation (R_c). T_m is the melting temperature, T_g is the glass-transition temperature and T_n and t_n are the temperature and time point at the locus, respectively (modified from Angell et al., 2008).

$$T_{rg} = \frac{T_g}{T_m} \tag{2}$$

The T_{rg} value is a predictor for the resistance to crystallisation: the higher the T_{rg} value, the higher the GFA (Turnbull, 1969), and presumably the glass stability.

Another parameter, the reduced temperature (T_{red}), is an indicator of crystallisation rate: the higher the T_{red} value, the lower the GFA (Zhou et al., 2002). T_{red} can be calculated as follows:

$$T_{red} = \frac{T_x - T_g}{T_m - T_g} \tag{3}$$

where T_x is the onset of crystallisation temperature observed during heating.

Amorphous solids are structurally and thermodynamically unstable and susceptible to partial or complete crystallisation upon storage (Bhugra et al., 2008; Karmwar et al., 2011; Miyazaki et al., 2007). Crystallisation of the amorphous form of a drug is undesirable as it will result in a lower dissolution rate and solubility of the drug and thus potentially in a lower bioavailability (Savolainen et al., 2009). Thus for the formulation scientist, it is important to consider the factors that are responsible for glass instability and also to have a better understanding of the parameters that may act as indicators of glass stability.

In this study we have initially determined the R_c of indomethacin and then calculated the GFA parameters T_{rg} and T_{red} for amorphous forms of indomethacin, cooled from the melt at various cooling rates above R_c, to investigate how different cooling rates affect these GFA parameters and if these correlate to the physical stability of the resulting amorphous forms of the drug (as an indicator for glass stability).

1.2. Kinetic analysis

As stated in the above section, GFA parameters may be used to estimate the glass stability of a material (in the current study as a function of different cooling rates). It is however, also possible to assess glass stability by evaluating the crystallisation tendency upon heating the glass above its T_g.

Thermally generated conversions can be explored by either isothermal or non-isothermal crystallisation methods (Málek, 2000). In isothermal mode, the amorphous sample is quickly brought to a particular temperature above or below the T_g and heat evolved during the crystallisation process is recorded as a function of time. In contrast, in non-isothermal techniques, the amorphous sample is heated at a constant rate and the heat evolved upon crystallisation is recorded as a function of temperature or time. A drawback of the isothermal methods however, is the impracticality of achieving the desired temperature immediately and, no measurements are possible in the period of time taken by the system to come to equilibrium (Starink and Zahra, 1997). Non-isothermal techniques do not have this drawback. This study deals with potential differences in thermal and structural properties based only on different cooling rates upon preparation. It is expected that these differences may be quite subtle, and for this reason, in the current study only non-isothermal techniques were used.

Most approaches describing a crystallisation process are based on the Avrami model of crystallisation (Augis and Bennett, 1978; Avrami, 1939, 1940, 1941). This model describes the time dependence of the fractional crystallisation α, usually written in the form:

$$\alpha = 1 - \exp[-(Kt)^n] \tag{4}$$

where K and n are constants. The rate equation can be obtained by differentiating Eq. 4 with respect to time, t:

$$\frac{d\alpha}{dt} = f(\alpha) = Kn(1-\alpha)[-\ln(1-\alpha)]^{1-\frac{1}{n}} \quad (5)$$

This equation is usually referred to as the Johnson–Mehl–Avrami (JMA) equation and in this form may be used for the thermal analysis of isothermal crystallisation events (Henderson, 1979). López-Alemany et al. (1999) have demonstrated the applicability of the JMA equation to non-isothermal crystallisation of glasses using the following equation:

$$\ln[-\ln(1-\alpha)] = -n\ln\beta + \ln C_0 - 1.052\frac{mE_a}{RT} \quad (6)$$

where α is the fraction crystallized, n is the Avrami kinetic exponent, m is the parameter of dimensionality of crystal growth, β is the heating rate, T is the temperature, R is the gas constant, C_0 represents a constant, and E_a is the apparent activation energy of crystal growth (E_a can be determined using Kissinger's method by plotting $ln(\beta/T_p^2)$ vs. $1/T_p$. The slope of the $ln(\beta/T_p^2)$ dependence on $1/T_p$ is equal to $-E_a/R$, where T_p is the peak temperature of the crystallisation event).In this form, the JMA equation is commonly used for analysis of non-isothermal crystallisation events even though this model may have restricted applicability for non-isothermal transformations involving nucleation and growth (Sessa et al., 1996; Yu and Lai, 1996). To verify whether the JMA model can be applied, two "tests" may be used (Adnađevic et al., 2010; Málek, 1995): (i) there should be a linear dependence of $ln[-ln(1-\alpha)]$ as a function of the reciprocal temperature, $1/T$ and (ii) the maximum values obtained for the functions $y(\alpha)$ and $z(\alpha)$ should be within certain ranges (see below). These functions can be defined in non-isothermal conditions as:

$$y(\alpha) = \varphi \exp\left(-\frac{E_a}{RT}\right) \quad (7)$$

$$z(\alpha) = \varphi T^2 \quad (8)$$

where φ is the heat flow normalized per mass of sample and can be written as:

$$\varphi = \Delta H_c A \exp\left(-\frac{E_a}{RT}\right) f(\alpha) \quad (9)$$

where ΔH_c is the total enthalpy of crystallisation, A is the pre-exponential factor, and the function $f(\alpha)$ is an algebraic expression of the JMA model (Eq. 5).

The validity of the JMA model for non-isothermal crystallisation can be verified by checking the maximum value (denoted as α_z^*) of the $z(\alpha)$ function (Eq. 8). If the maximum value falls within the range of $0.61 \leqslant \alpha_z^* \leqslant 0.65$ (Málek, 1992; Sesták and Berggren, 1971), then the experimental data correspond to the JMA model. In contrast, if the value of α_z^* is not in the range of 0.61–0.65 and the maximum value of the $y(\alpha)$ function (Eq. 7) (denoted as α_y^*) is in the range of 0–α_z^*, then the experimental data may be better described by the autocatalytic Sestak-Berggren (SB) model (Sesták and Berggren, 1971). The autocatalytic SB model (Málek, 1992, 2000; Sesták and Berggren, 1971) can be defined as:

$$f(\alpha) = \alpha^M(1-\alpha)^N \quad (10)$$

where $f(\alpha)$ is corresponding to the crystallised fraction, and M and N are kinetic exponents describing the relative contributions of acceleratory and decay regions of the kinetic process. For the autocatalytic SB model, the ratio of the kinetic exponent M/N can be written as (Pustková et al., 2007):

$$\frac{M}{N} = \frac{\alpha_y^*}{1-\alpha_y^*} \quad (11)$$

where α_y^* corresponds to the maximum of the $y(\alpha)$ function.

Taking into account the basic kinetic equation for non-isothermal conditions (Adnađevic et al., 2010):

$$\beta\frac{d\alpha}{dT} = k(T)f(\alpha) \quad (12)$$

where β is the heating rate, $k(T)$ is the temperature dependent rate constant ($k(T) = A\exp(-E_a/RT)$), and $f(\alpha)$ is the conversion function given by Eq. 10, the autocatalytic SB kinetic equation can be written as (Málek, 2000):

$$\ln\left[\beta\left(\frac{d\alpha}{dT}\right)\exp\left(-\frac{E_a}{RT}\right)\right] = \ln A + N\ln[\alpha^{\frac{M}{N}}(1-\alpha)] \quad (13)$$

The kinetic exponent N can be obtained by the slope of the linear dependence of $ln[\beta(d\alpha/dT)exp(Ea/RT)]$ and $ln[\alpha^{M/N}(1-\alpha)]$, and the value of M can then be obtained using Eq. 11.The kinetic exponents M and N can be linked to the complexity of the crystallisation process (with higher values for both M and N denoting higher rates of nucleation and higher overlapping of nuclei in the crystallisation process respectively).

In this study we have applied the JMA and autocatalytic SB model to the crystallisation of amorphous forms of indomethacin, cooled from the melt at various cooling rates above R_c, to investigate which model could be applied and to link parameters of these model to glass stability.

The overall aims of this study were:

- to investigate whether amorphous indomethacin prepared using different cooling rates above the R_c (determined by a TTT diagram) exhibit different structural characteristics (investigated by Raman spectroscopy),
- to establish a correlation between the cooling rate and GFA (T_{rg} and T_{red}) for amorphous indomethacin prepared at various cooling rates and glass stability (determined as the time to crystallisation), and
- to describe the non-isothermal crystallisation kinetics of amorphous indomethacin prepared using different cooling rates (investigated by differential scanning calorimetry) and to link parameters of these models to glass stability (determined as the time to crystallisation).

2. Materials and methods

2.1. Materials

The γ-form of indomethacin (98%) was purchased from Chemie Brunschwig AG (Basel, Switzerland) and was used as received after verification of the polymorphic form by XRPD.

2.2. Preparation of amorphous samples

Indomethacin (γ-form) was melted in a stainless steel beaker at 165 °C for 3 min. The melt was then transferred into DSC pans (TA Instruments, New Castle, USA). These DSC pans were subsequently cooled at different cooling rates (1.2, 3, 5, 7, 10, 20 and 30 K min^{-1}) above the R_c of indomethacin (see Section 2.3.2) in a DSC instrument (DSC Q100, TA Instruments, New Castle, USA). The resulting amorphous solids were stored in a desiccator over P_2O_5 at 22 ± 0.2 °C. Samples were prepared in triplicate.

2.3. Characterisation

The freshly prepared and stored samples were characterized using the following techniques (freshly prepared samples were analysed within one hour of preparation):

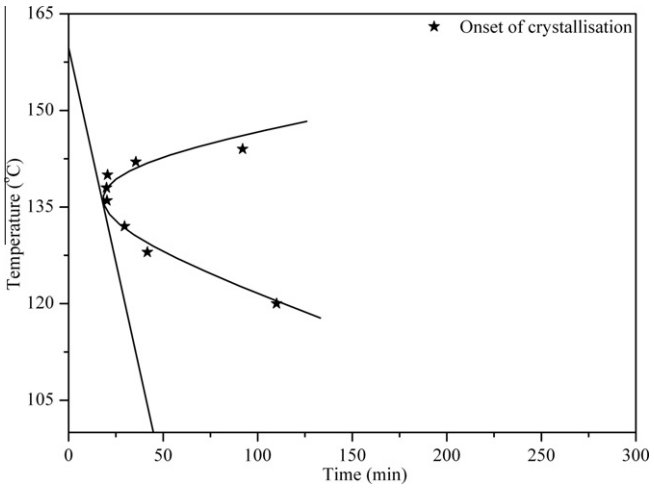

Fig. 2. TTT-diagram showing the minimum cooling rate required to obtain amorphous indomethacin (solid line).

2.4. Determination of the TTT diagram of indomethacin

TTT diagram was determined by using a differential scanning calorimetry (DSC) instrument (DSC Q100 calorimeter, V8.2 Build 268, TA Instruments, New Castle, USA) under a nitrogen gas flow of 50 mL min^{-1}. Approximately 2–5 mg of γ-indomethacin were crimped into aluminium pans, heated to 165 °C, held isothermal for 3 min and then cooled at a rate of 20 K min^{-1} to predetermined temperatures (144, 142, 140, 138, 136, 132, 130, and 120 °C) below the melting temperature of γ-indomethacin (T_m = 159 °C). Samples were then kept isothermal at the predetermined temperatures below the T_m and the time to re-crystallisation was determined.

To validate the TTT diagram, approximately 2–5 mg of γ-indomethacin was heated to 165 °C in the DSC instrument. Samples were then cooled to 20 °C at different cooling rates above and below R_c (20, 10, 6, 7, 5, 3, 1.2, 1.0, 0.3, 0.2, and 0.1 K min^{-1}) and allowed to equilibrate for 1 min. Samples were then reheated at 10 K min^{-1} to determine whether the resulting material was amorphous or crystalline.

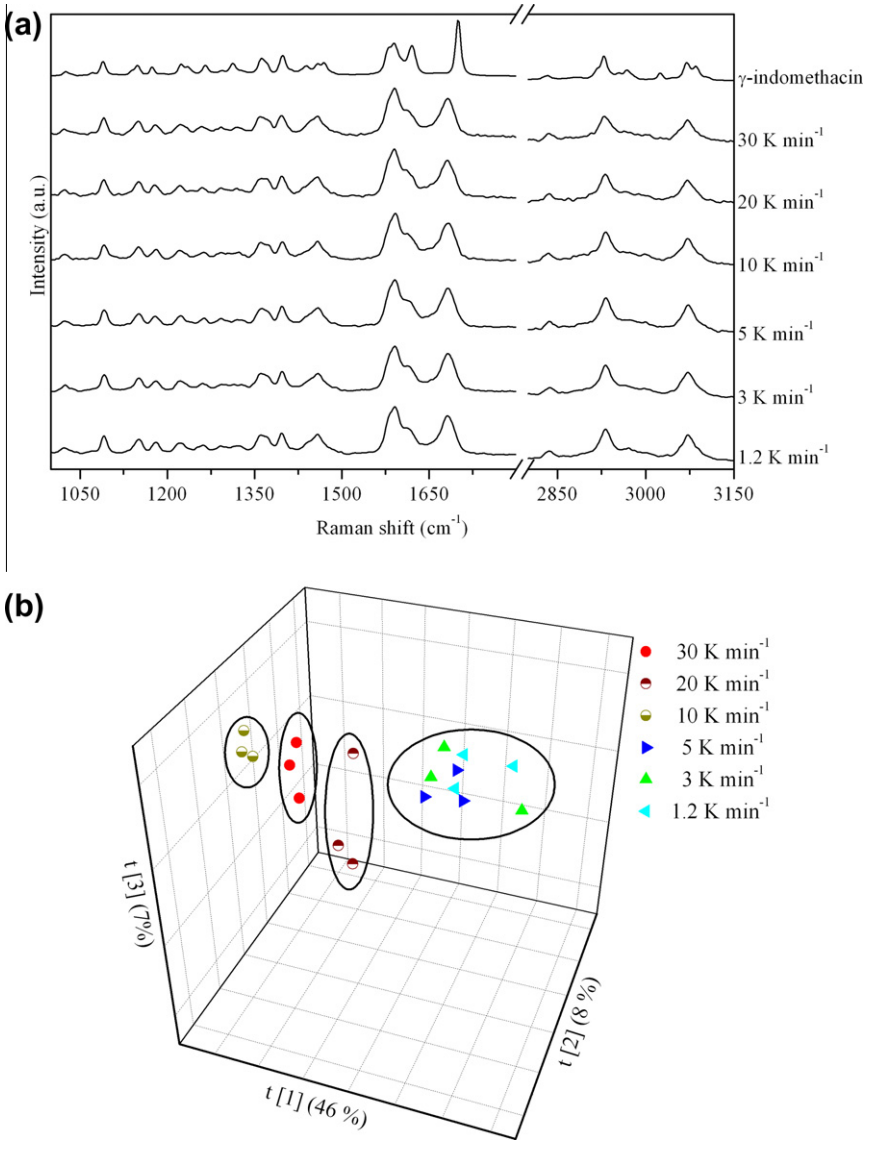

Fig. 3. (a) Raman spectra of amorphous samples of indomethacin, prepared from melts cooled at various cooling rates and (b) the corresponding PCA scores plot.

2.4.1. Structural characterisation of amorphous forms of indomethacin

X-ray powder diffraction (XRPD): Samples were analysed with a PANalytical X'Pert PROMPD system (PW3040/60, Philips, The Netherlands) using Cu Kα radiation with $\lambda = 1.542$ Å and a divergence slit of 1°. The samples were gently consolidated in a flat aluminium sample holder and scanned at 40 kV and 30 mA from 5° to 35° 2θ using a scanning speed of 0.1285°min^{-1} and a step size of 0.0084°. The diffraction patterns were generated using X'Pert High Score Version 2.2.0 (Philips, The Netherlands).

Raman spectroscopy: The FT-Raman instrument consisted of a Bruker FRA 106/S FT-Raman accessory (Bruker Optik, Ettlingen, Germany) with a Coherent Compass 1064–500 N laser (Coherent Inc., Santa Clara, USA) attached to a Bruker Equinox 55 FT interferometer, and a D 418T liquid nitrogen cooled Ge diode detector. All measurements were carried out at room temperature utilizing a laser wavelength of 1064 nm (Nd:YAG laser). Spectra were the average of 128 scans, taken at a resolution of 4 cm^{-1} with a laser power of 120 mW.

Principal component analysis (PCA) was used to help interpret differences in the Raman spectra of the differently cooled amorphous forms. Prior to PCA, standard normal variant (SNV) transformation was performed on the spectra to remove intensity differences unrelated to the sample composition and the spectra were then mean centered. PCA was performed on the spectral ranges from 1000 to 1720 cm^{-1} and 2800 to 3100 cm^{-1}. PCA and spectral preprocessing and scaling were performed using The Unscrambler Software Version 9.8 (CAMO Software AS, Oslo, Norway).

2.5. Stability study

The freshly prepared amorphous samples were stored at 22 °C ± 0.2 °C over P_2O_5. Upon storage, the differently cooled indomethacin melts were investigated by polarizing light microscopy (Motic BA300pol, BA series, Motic Incorporation Ltd., Hong Kong, China), equipped with cross polars, a 360° rotatable stage and a variable 30 W/6 V halogen light source). Images were taken using a Moticam 2300 digital camera with a resolution of three megapixels and a minimum illumination of three Lux. Images were taken at regular intervals for all the stored samples and the time to appearance of birefringence was taken as the onset time of crystallisation.

2.6. Determination of GFA and non-isothermal crystallisation parameters

GFA parameters were calculated as outlined in the introduction on the basis of DSC measurements. Approximately 2–5 mg of freshly prepared amorphous samples were crimped in an aluminium pan and heated at a rate of 10 K min^{-1} from 0 to 180 °C under a nitrogen gas flow of 50 mL min^{-1}. The glass transition temperature (T_g), crystallisation temperature (T_c) and melting temperature (T_m) were determined using TA Universal Analysis Software (Version 4.0C). The T_g was defined as the midpoint of the change in heat capacity of the sample, while both T_c and T_m were defined using the onset temperatures of the exothermic and endothermic events, respectively.

Non-isothermal crystallisation experiments were performed by heating the samples at a heating rate of 10 K min^{-1}. The exothermic event was recorded as a function of temperature and kinetic exponents M and N were calculated as outlined in the Section 1.

Analysis of variance (ANOVA) was performed on the thermal events using Microsoft Excel Software (MS Office 2007, Microsoft Corporation, Washington, USA).

3. Results and discussion

3.1. Determination of the TTT diagram of indomethacin

The characteristic "nose" shape of the region of nucleation and crystal growth in the TTT diagram is a result two opposing driving forces as a function of increasing temperature: a decreased driving

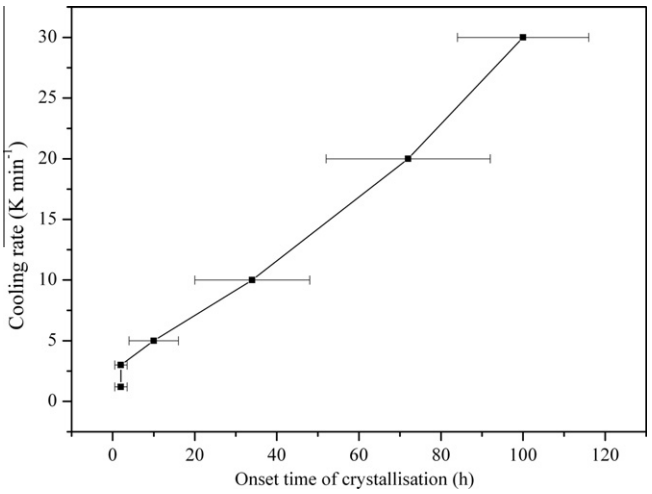

Fig. 4. Onset time of crystallisation for amorphous samples of indomethacin prepared from melts cooled at various cooling rates and stored at T_g −20 °C.

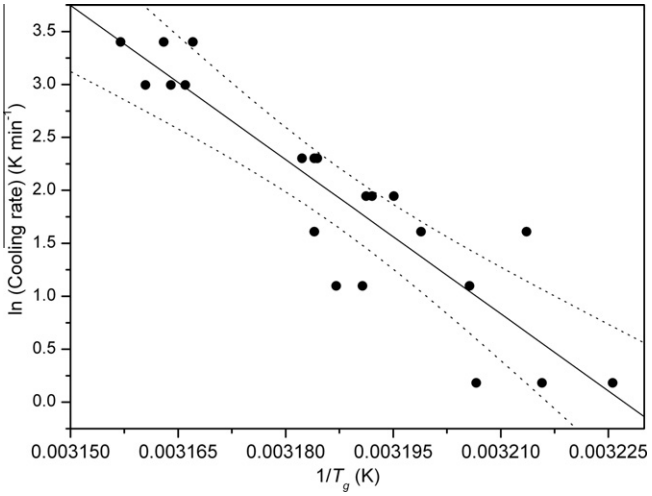

Fig. 5. Influence of cooling rate of indomethacin melts on the glass transition temperature of the resulting amorphous forms (95% confidence interval is shown as dotted line and solid line is a linear regression fit).

Table 1
Thermal properties (glass transition temperature, T_g and crystallisation temperature, T_c) of melts of indomethacin cooled at various cooling rates.

Cooling rate (K min^{-1})	T_g (°C)	$T_{c,\ ons}$ (°C)
30	43.9 ± 0.58	109.8 ± 2.28
20	43.2 ± 0.17	110.7 ± 3.13
10	41.0 ± 0.11	110.7 ± 2.84
7	40.1 ± 0.20	109.4 ± 3.04
5	39.5 ± 1.44	110.0 ± 3.53
3	39.9 ± 0.96	110.4 ± 3.22
1.2	37.8 ± 0.92	109.8 ± 2.76

force for crystallisation and an increased effective diffusivity of the material (Busch, 2000; Wen et al., 2008). The "tip of the nose" is usually referred to as the locus. The TTT diagram for indomethacin was constructed from several isothermal DSC thermograms and is shown in Fig. 2. R_c was calculated as the rate tangential to the nose of the TTT diagram with an onset from the melting point of the material (159 °C). The locus position observed for indomethacin was at approximately 138 °C and after 20 min, corresponding to a minimum cooling rate of 1.2 K min^{-1}.

For inorganic materials, R_c has also been estimated by an experimental method developed by Barandiaran and Colmenoro (1981), in which a relationship between the difference of melting temperature and the peak temperature of crystallisation (T_m–$T_{c,\ peak}$) and the cooling rate (q) was shown using the following equation:

$$\ln(q) = A - \frac{B}{(T_m - T_{c,\ peak})^2} \tag{14}$$

where A and B represent the intercept and slope of the linear dependence of $ln(q)$ against $1/(T_m–T_{c,\ peak})^2$.

Using the values of A and B, Cabral et al. (2003) predicted R_c as:

$$R_c = \exp\left(A - \frac{B}{T_m^2}\right) \tag{15}$$

Calculations based on Eqs. 14 and 15 are in good agreement with the experimental values derived from the TTT diagram. The predicted and the experimental R_c values for indomethacin were 1.0 and 1.2 K min^{-1}, respectively. This approach to evaluate the R_c has mostly been used for inorganic materials (Cabral et al., 2003; Whichard and Day, 1984). The current finding however, suggests that this approach may also be applicable to other organic materials. However, further detailed investigations with a range of organic materials are needed."

As stated earlier, cooling rates that traverse through the "nose" of the TTT diagram must lead to re-crystallisation of the amorphous drug during cooling. In order to validate this, several continuous cooling transformation (CCT) experiments were performed with cooling rates above and below the calculated R_c. The DSC thermograms from samples with a cooling rate higher than R_c (cooling rates of 20, 10, 6, 3 K min^{-1}) showed that the indomethacin was indeed amorphous and exhibited a T_g as the only thermal event. In contrast, in the DSC thermograms of samples with a cooling rate lower than R_c (cooling rates of 1, 0.3, 0.2, 0.1 K min^{-1}) no T_g was

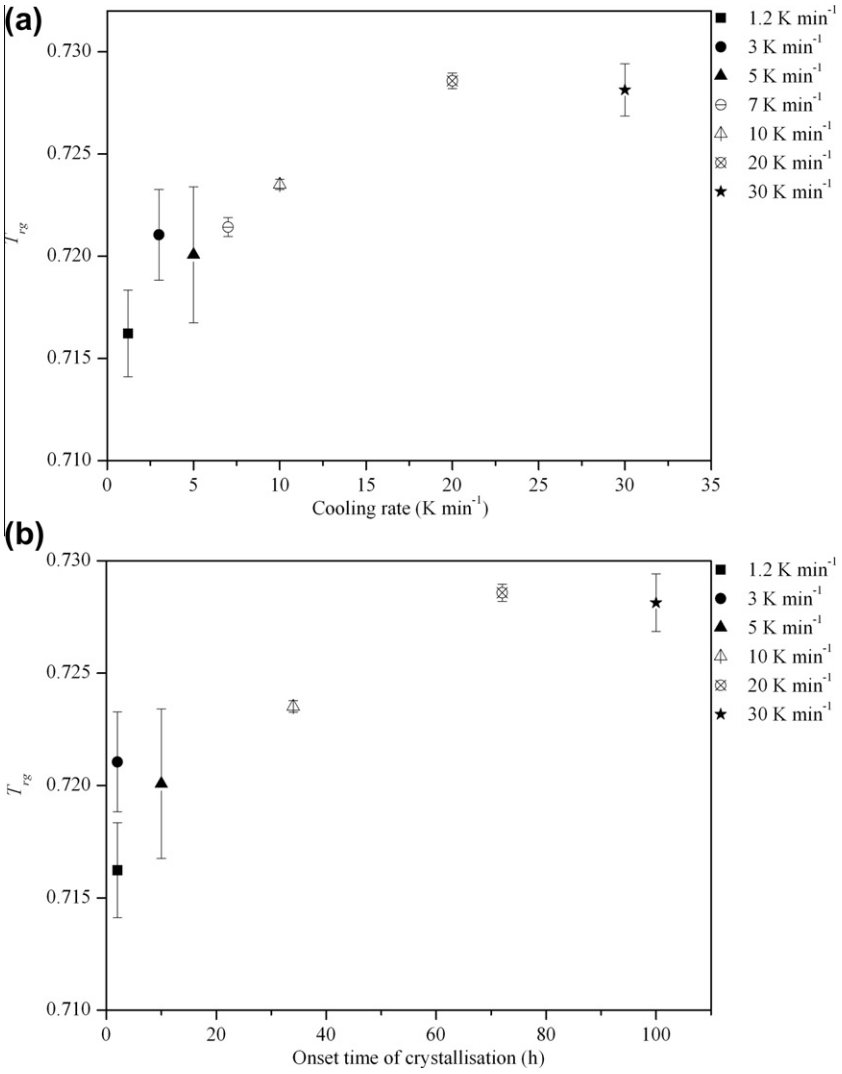

Fig. 6. Reduced glass transition temperature (T_{rg}), (a) as a function of the cooling rate and (b) as a function of onset time of crystallisation for differently cooled amorphous indomethacin samples.

observed, but two endothermic events at 155 and 159 °C, corresponding to melting of the crystalline α and γ form of indomethacin, respectively. Therefore, the R_c required to obtain amorphous indomethacin was in agreement with the experimentally obtained R_c of 1.2 K min^{-1}.

3.2. Structural characterisation of amorphous forms of indomethacin

A complete lack of diffraction peaks in the diffractograms for the differently cooled samples at cooling rates above R_c (30, 20, 10, 7, 5, 3 and 1.2 K min^{-1}) revealed that indomethacin was X-ray amorphous regardless of the cooling rate. The diffractograms of the differently cooled samples showed only a halo with a broad maximum around 21° 2θ (data not shown). These data were reproducible for three batches from each preparation method.

Raman spectroscopy, as a molecular level technique, was performed on the same samples to assist in understanding possible structural differences between the samples. The Raman spectra of all freshly prepared amorphous samples contained peaks that were broader and more merged than those of the crystalline γ-form (Fig. 3(a)), which is due to the inherent variations in molecular conformation and intermolecular bonding in the amorphous form. There were several peak position differences between the amorphous and crystalline forms, which have previously been observed (Savolainen et al., 2007; Strachan et al., 2007), but no spectral features resembling the α- or γ-forms for any of the amorphous samples.

As the spectra of the differently cooled amorphous forms were fairly similar, PCA was used to investigate spectral variation in the SNV transformed and mean-centred data. The scores plot (Fig. 3(b)) was used to investigate differences between the differently cooled samples based on the PCA model. 61% of the variation in the SNV transformed and centred data was explained by the first three principal components (PCs). The spectra of triplicate samples clustered in the scores plot according to the cooling rate, suggesting that structural differences are indeed present and reproducible. In the scores plot, the samples cooled with 1.2, 3 and 5 K min^{-1} clustered together. In contrast, samples cooled with 10, 20 and 30 K min^{-1} were slightly resolved from each other.

The largest spectral differences were observed in the regions from 1540 to 1700 cm^{-1} and from 2930 to 3100 cm^{-1}. The main vibrations associated with the bands in these regions have previ-

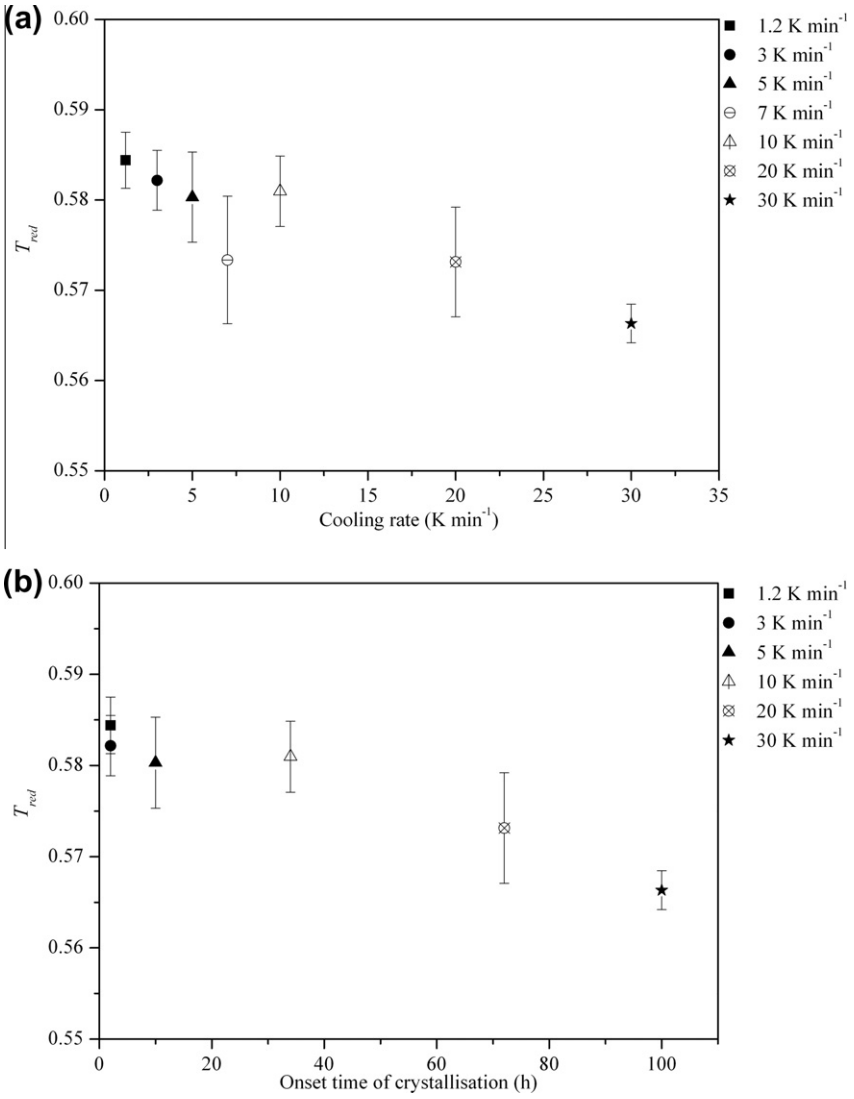

Fig. 7. Reduced temperature (T_{red}), (a) as a function of the cooling rate and (b) as a function of onset time of crystallisation for differently cooled amorphous indomethacin samples.

ously been assigned for quench cooled amorphous indomethacin as follows: in-plane indole ring deformation (1580 cm^{-1}), chlorobenzoyl ring deformation (1591 cm^{-1}), C–O stretching associated with indole ring deformation (1613 cm^{-1}), benzoyl C=O stretching (1681 cm^{-1}), and aliphatic (2930 and 2970 cm^{-1}) and aromatic C–H stretching (3000 to 3100 cm^{-1}) (Strachan et al., 2007; Savolainen et al., 2007). The range of vibrations associated with the largest spectral differences suggests that the systematic differences were due to a range of molecular conformations and intermolecular interactions associated with the different cooling rates.

3.3. Stability study

The freshly prepared differently cooled melts of indomethacin showed no birefringence, suggesting complete absence of crystallinity. PLM was thus used to monitor the onset of crystallisation for all differently cooled amorphous samples (at cooling rates above R_c). Upon storage, birefringence was observed after different time periods for the different samples. The 1.2 and 3 K min^{-1} cooled samples crystallised the fastest (<1 h) and the samples cooled with 30 K min^{-1} crystallised the slowest (<130 h). The ranking of stability for the differently cooled samples was 30 K min^{-1} > 20 K min^{-1} > 10 K min^{-1} > 5 K min^{-1} > 3 K min^{-1} - ≈ 1.2 K min^{-1} (Fig. 4).

3.4. Determination of GFA and non-isothermal parameters

From the DSC thermograms, a significant increase in T_g for the amorphous samples as a function of increased cooling rate was found (Fig. 5 and Table 1). In contrast, the onset of crystallisation temperature showed no significant differences with the change in cooling rate (Table 1).

To investigate differences in GFA for differently cooled samples, the value for the reduced glass transition temperature (T_{rg}) for the differently cooled samples was calculated. According to the nucleation theory (Turnbull, 1949), a liquid with a high viscosity between T_g and T_m, exhibits a high GFA with a low R_c. It was postulated that a high value of the T_{rg} for amorphous indomethacin would result in a higher viscosity in the supercooled liquid state at a given temperature and thus better inhibit nucleation and subsequent crystal growth. Also, according to Lu and Liu, the higher the T_{rg}, the higher the viscosity of the melt, before it is supercooled and consequently, the lower the possibility of crystallisation (Lu and Liu, 2002). This will improve GFA, and presumably, glass stability. Since the T_g of amorphous indomethacin increased with increasing cooling rate, but T_m stays constant, T_{rg} was also found to increase (Fig. 6(a)). For indomethacin the data shows that an increase in T_{rg} indeed corresponds to an increase in glass stability (Fig. 6(b)).

In contrast to the T_{rg}, the value of another GFA parameter T_{red} (reduced temperature), decreases with an increase in cooling rate (Fig. 7(a)). T_{red} provides a basis for comparing the ease of crystallisation (i.e. how far an amorphous sample can be heated above T_g before crystallisation takes place) of compounds with different T_{gs} (Gupta et al., 2004), and was thus used in this study, as the T_{gs} of the indomethacin samples differed as a function of the cooling rate. The relative ease of crystallisation in this study follows the order:
1.2 K min^{-1} > 3 K min^{-1} > 5 K min^{-1} > 10 K min^{-1} > 20 K min^{-1} > 30 K min^{-1}. This was expected, as T_{red} is an indicator of crystallisation rate: the higher the T_{red} value, the lower the GFA (Zhou et al., 2002). However, T_{red} showed a weaker correlation with the relative glass stability of the differently cooled samples, compared to T_{rg} (Fig. 7(b)).

To determine non-isothermal parameters, the crystallisation behaviour upon heating of the differently cooled samples was studied. First the Johnson–Mehl–Avrami (JMA) model was used. The volume fraction α crystallized at any temperature T is given

Table 2
Values of α_y^* and α_z^* for the non-isothermal crystallisation process of melts of indomethacin cooled at various cooling rates.

Cooling rate (K min^{-1})	α_y^*	α_z^*
30	0.39 ± 0.01	0.43 ± 0.02
20	0.40 ± 0.01	0.43 ± 0.02
10	0.39 ± 0.02	0.42 ± 0.01
5	0.38 ± 0.02	0.43 ± 0.02
3	0.40 ± 0.02	0.42 ± 0.02

Table 3
Values of the kinetic exponents M and N of the autocatalytic SB model for the non-isothermal crystallisation process of melts of indomethacin cooled at various cooling rates.

Cooling rate (K min^{-1})	M	N
30	0.49 ± 0.03	0.74 ± 0.28
20	0.52 ± 0.02	0.82 ± 0.12
10	0.74 ± 0.14	1.27 ± 0.25
5	0.76 ± 0.11	1.02 ± 0.19
3	1.01 ± 0.12	1.44 ± 0.17

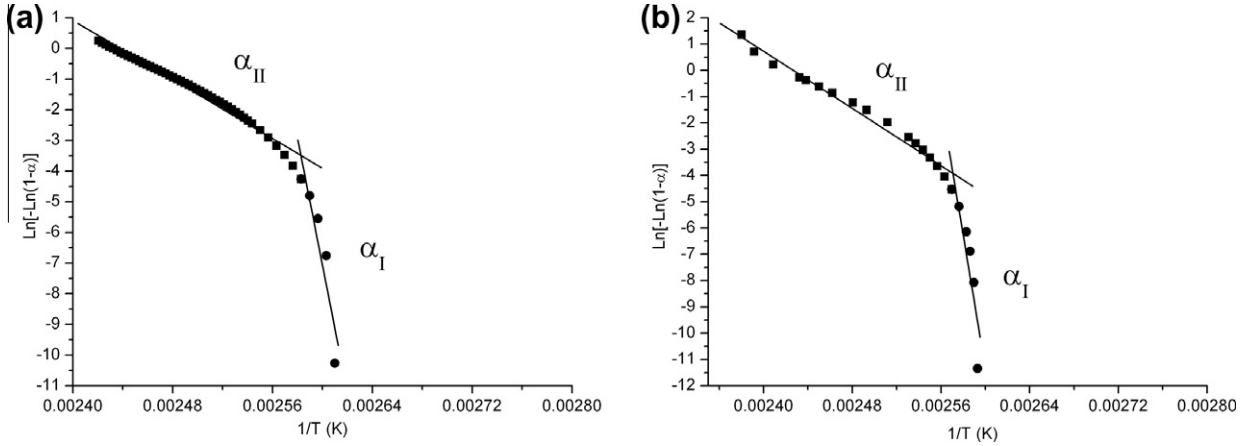

Fig. 8. $ln[ln(1-\alpha)]$ versus $1/T$ plot of differently cooled samples. (a) Melt cooled at a rate of 30 K min^{-1}, (b) melt cooled at a rate of 3 K min^{-1}. Linear regression analysis was applied to fit a line through the two distinct regions of α, denoted as α_I and α_{II}.

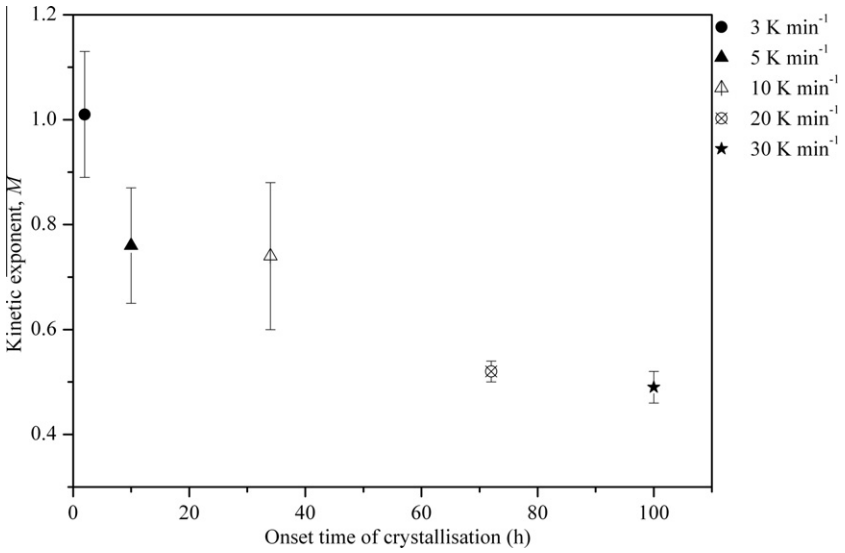

Fig. 9. Kinetic exponent M (autocatalytic SB model) as a function of onset time of crystallisation for differently cooled amorphous indomethacin samples.

by $\alpha = A_T/A$ (A is the total area of the exothermic peak between T_c and end of crystallisation temperature and A_T is the partial area of the exothermic peak from T_c to T). In order to check if the JMA model for the non-isothermal crystallisation is applicable in this study, the dependence of $ln[-ln(1-\alpha)]$ against $1/T$ was investigated (Fig. 8). Fig. 8 demonstrates for two differently cooled samples that $\ln[-ln(1-\alpha)]$ vs $1/T$ was not linear over the entire reciprocal temperature range. Rather, the presence of two separate regions (α_I and α_{II}) was found. Similar results were found for all differently cooled samples, indicating that the JMA non-isothermal kinetic model may not describe the transformation behaviour of differently cooled samples over the entire temperature range studied. To further confirm this, the $y(\alpha)$ and $z(\alpha)$ functions (Eqs. 7 and 8) were plotted for all samples. The value of α_y^* (maximum value) of the $y(\alpha)$ function was in the range of 0–α_y^* (maximum value) and the value of α_z^* of $z(\alpha)$ function was in the range of 0.38–0.43 (Table 2). Therefore, α_z^* was clearly outside the characteristic range of $0.61 \leqslant \alpha_z^* \leqslant 0.65$ for the JMA kinetic model.

The JMA model is valid in non-isothermal conditions provided that a new crystalline phase grows from a constant number of nuclei and all nucleation is completed before the macroscopic crystal growth starts (Henderson, 1979). It thus seems that the nucleation and growth processes are probably overlapping for the differently cooled amorphous indomethacin samples and the overall crystallisation cannot be described by the JMA model.

From the values obtained for the $y(\alpha)$ and $z(\alpha)$ functions, it can be concluded that the non-isothermal crystallisation kinetic of differently cooled samples may be explained by the two-parameter autocatalytic SB kinetic model. The values of the kinetic exponents M and N were obtained from Eqs. 11 and 12 and are listed in Table 3. The kinetic exponent M indicates an important role of the crystallized phase on the overall crystallisation kinetic, whilst N is indicative for an increased complexity of the process, correlated to the overlapping of the nuclei (Adnađevic et al., 2010; Málek, 2000). It can be noted that the value of M decreases as a function of cooling rate. In contrast, no trend was observed for the kinetic exponent N with respect to cooling rates employed in this study. The kinetic exponent M also correlates with the stability of the differently cooled samples (Fig. 9) and may thus be used as an indicator of glass stability. It may be speculated that decreasing cooling rates lead to a higher number of nuclei in the resulting amorphous material, since it has been in the super cooled state for a longer time period.

4. Conclusions

In this study it was demonstrated that amorphous indomethacin could be prepared by cooling the melt at a minimum cooling rate of $1.2\,K\,min^{-1}$. Differently cooled melts of indomethacin showed differences on the molecular level (detected by Raman spectroscopy). The GFA determined for all samples using the T_{rg} and T_{red} approach where values were determined above the T_g correlated with the experimentally determined physical stability of the samples stored at temperatures below the T_g. The JMA model could not be used to explain the complex, non-isothermal crystallisation of this amorphous drug. The non-isothermal crystallisation kinetic of all the differently cooled samples was best described by the autocatalytic SB model. Differences in the non-isothermal crystallisation processes for the differently cooled samples may be governed by nucleation (number of nuclei). The values of the kinetic exponent, M, for the differently cooled samples, can be correlated to their stability. The findings in this study, from a practical point of view, may not only be important to optimise physical stability of amorphous forms, but may also have consequences for the dissolution behaviour (and thus potentially for the bioavailability) of differently prepared amorphous materials. This is the topic of ongoing investigation.

References

Adnađevic, B., Jankovic, B., Minic, D.M., 2010. Kinetics of the apparent isothermal and non-isothermal crystallization of the [alpha]-Fe phase within the amorphous Fe81B13Si4C2 alloy. J. Phys. Chem. Solids 71, 927–934.

Angell, A.C., 2008. Glass-formers and viscous liquid slowdown since David Tumbull: Enduring Puzzles and New Twists. Materials Research Society, Warrendale, PA, ETATS-UNIS.

Augis, J.A., Bennett, J.E., 1978. Calculation of the Avrami parameters for heterogeneous solid state reactions using a modification of the Kissinger method. J. Therm. Anal. Calorim. 13, 283–292.

Avrami, M., 1939. Kinetics of phase change. I general theory. J. Chem. Phys. 7, 1103–1112.

Avrami, M., 1940. Kinetics of phase change. II transformation-time relations for random distribution of nuclei. J. Chem. Phys. 8, 212–224.

Avrami, M., 1941. Granulation, phase change, and microstructure kinetics of phase change III. J. Chem. Phys. 9, 177–184.

Barandiarán, J.M., Colmenero, J., 1981. Continuous cooling approximation for the formation of a glass. J. Non-Cryst. Solids 46, 277–287.

Bhugra, C., Shmeis, R., Pikal, M.J., 2008. Role of mechanical stress in crystallization and relaxation behavior of amorphous indomethacin. J. Pharm. Sci. 97, 4446–4458.

Bøtker, J.P., Karmwar, P., Strachan, C.J., Cornett, C., Tian, F., Zujovic, Z., Rantanen, J., Rades, T., 2011. Assessment of crystalline disorder in cryo-milled samples of

indomethacin using atomic pair-wise distribution functions. Int. J. Pharm. 417, 112–119.
Busch, R., 2000. The thermophysical properties of bulk metallic glass-forming liquids. J. Min. Met. Mat. Soc. 52, 39–42.
Cabral, A.A., Cardoso, A.A.D., Zanotto, E.D., 2003. Glass-forming ability versus stability of silicate glasses. I. Experimental test. J. Non-Cryst. Solids 320, 1–8.
Denicourt, T., Hedoux, A., Guinet, Y., Willart, J.F., Descamps, M., 2003. Raman scattering investigations of the stable and metastable phases of cyanoadamantane glassy crystal. J. Phys. Chem. B 107, 8629–8636.
Giordano, M., Russo, M., Capoluongo, P., Cusano, A., Nicolais, L., 2005. The effect of cooling rate on the glass transition of an amorphous polymer. J. Non-Cryst. Solids 351, 515–522.
Graeser, K.A., Patterson, J.E., Rades, T., 2009. Applying thermodynamic and kinetic parameters to predict the physical stability of two differently prepared amorphous forms of simvastatin. Curr. Drug Deliv. 6, 374–382.
Gupta, P., Chawla, G., Bansal, A.K., 2004. Physical stability and solubility advantage from amorphous celecoxib: the role of thermodynamic quantities and molecular mobility. Mol. Pharm. 1, 406–413.
Hancock, B.C., Shalaev, E.Y., Shamblin, S.L., 2002. Polyamorphism: a pharmaceutical science perspective. J. Pharm. Pharmacol. 54, 1151–1152.
Heinz, A., Strachan, C.J., Atassi, F., Gordon, K.C., Rades, T., 2007. Characterizing an amorphous system exhibiting trace crystallinity: a case study with saquinavir. Cryst. Growth Des. 8, 119–127.
Henderson, D.W., 1979. Thermal analysis of non-isothermal crystallization kinetics in glass forming liquids. J. Non-Cryst. Solids 30, 301–315.
Hng, H.H., Li, Y., Ng, S.C., Ong, C.K., 1996. Critical cooling rates for glass formation in Zr-Al-Cu-Ni alloys. J. Non-Cryst. Solids 208, 127–138.
Karmwar, P., Graeser, K., Gordon, K.C., Strachan, C.J., Rades, T., 2011. Investigation of properties and recrystallisation behaviour of amorphous indomethacin samples prepared by different methods. Int. J. Pharm. 417, 94–100.
Kaushal, A.M., Bansal, A.K., 2008. Thermodynamic behavior of glassy state of structurally related compounds. Eur. J. Pharm. Biopharm. 69, 1067–1076.
Kauzmann, W., 1948. The Nature of the Glassy state and the behavior of liquids at low temperatures. Chem. Rev. 43, 219–256.
López-Alemany, P.L., Vázquez, J., Villares, P., Jiménez-Garay, R., 1999. Kinetic study on non-isothermal crystallization in glassy materials: application to the Sb0.12As0.40Se0.48 alloy. J. Alloys Compd 285, 185–193.
Lu, Z.P., Liu, C.T., 2002. A new glass-forming ability criterion for bulk metallic glasses. Acta Mater. 50, 3501–3512.
Málek, J., 1992. The kinetic analysis of non-isothermal data. Thermochim. Acta 200, 257–269.
Málek, J., 1995. The applicability of Johnson-Mehl-Avrami model in the thermal analysis of the crystallization kinetics of glasses. Thermochim. Acta 267, 61–73.
Málek, J., 2000. Kinetic analysis of crystallization processes in amorphous materials. Thermochim. Acta 355, 239–253.
Miyazaki, T., Yoshioka, S., Aso, Y., Kawanishi, T., 2007. Crystallization rate of amorphous nifedipine analogues unrelated to the glass transition temperature. Int. J. Pharm. 336, 191–195.
Nascimento, M.L.F., Souza, L.A., Ferreira, E.B., Zanotto, E.D., 2005. Can glass stability parameters infer glass forming ability? J. Non-Cryst. Solids 351, 3296–3308.
Onorato, P.I.K., Uhlmann, D.R., 1976. Nucleating heterogeneities and glass formation. J. Non-Cryst. Solids 22, 367–378.
Patterson, J.E., James, M.B., Forster, A.H., Lancaster, R.W., Butler, J.M., Rades, T., 2005. The influence of thermal and mechanical preparative techniques on the amorphous state of four poorly soluble compounds. J. Pharm. Sci. 94, 1998–2012.
Pustková, P., Zmrhalová, Z., Málek, J., 2007. The particle size influence on crystallization kinetics of (GeS2)0.1(Sb2S3)0.9 glass. Thermochim. Acta 466, 13–21.
Savolainen, M., Heinz, A., Strachan, C., Gordon, K.C., Yliruusi, J., Rades, T., Sandler, N., 2007. Screening for differences in the amorphous state of indomethacin using multivariate visualization. Eur. J. Pharm. Sci. 30, 113–123.
Savolainen, M., Kogermann, K., Heinz, A., Aaltonen, J., Peltonen, L., Strachan, C., Yliruusi, J., 2009. Better understanding of dissolution behaviour of amorphous drugs by in situ solid-state analysis using Raman spectroscopy. Eur. J. Pharm. Biopharm. 71, 71–79.
Sessa, V., Fanfoni, M., Tomellini, M., 1996. Validity of Avrami's kinetics for random and nonrandom distributions of germs. Phys. Rev. B: Condens. Matter 54, 836.
Sesták, J., Berggren, G., 1971. Study of the kinetics of the mechanism of solid-state reactions at increasing temperatures. Thermochim. Acta 3, 1–12.
Starink, M.J., Zahra, A.M., 1997. Determination of the transformation exponent s from experiments at constant heating rate. Thermochim. Acta 298, 179–189.
Stillinger, F.H., Weber, T.A., 1984. Packing structures and transitions in liquids and solids. Science 225, 983–989.
Strachan, C.J., Rades, T., Gordon, K.C., 2007. A theoretical and spectroscopic study of γ-crystalline and amorphous indometacin. J. Pharm. Pharmacol. 59, 261–269.
Surana, R., Pyne, A., Suryanarayanan, R., 2004. Effect of preparation method on physical properties of amorphous trehalose. Pharm. Res. 21, 1167–1176.
Turnbull, D., 1969. Under what conditions can a glass be formed? Contemp. Phys. 10, 473–488.
Turnbull, D., Fisher, J.C., 1949. Rate of nucleation in condensed systems. AIP.
Wales, D.J., 2010. Energy landscapes of clusters bound by short-ranged potentials. Chem. Phys. Chem. 11, 2491–2494.
Wen, G.-H., Liu, H., Tang, P., 2008. CCT and TTT diagrams to characterize crystallization behavior of mold fluxes. J. Iron Steel Res., International 15, 32–37.
Whichard, G., Day, D.E., 1984. Glass formation and properties in the gallia-calcia system. J. Non-Cryst. Solids 66, 477–487.
Woodard, P.R., Chandrasekar, S., Yang, H.T.Y., 1999. Analysis of temperature and microstructure in the quenching of steel cylinders. Metall. Mater. Trans. B 30, 815–822.
Yu, G., Lai, J.K.L., 1996. Kinetics of transformation with nucleation and growth mechanism: Two- and three-dimensional models. J. Appl. Phys. 79, 3504.
Zhou, D., Zhang, G.G.Z., Law, D., Grant, D.J.W., Schmitt, E.A., 2002. Physical stability of amorphous pharmaceuticals: Importance of configurational thermodynamic quantities and molecular mobility. J. Pharm. Sci. 91, 1863–1872.